mathematics

MDPI

Article

The $\mathcal{T}_e$ Transform: A High-Resolution Integral Transform and Its Key Properties

Eduardo Trutié-Carrero [1], Diego Seuret-Jiménez [1,*], José M. Nieto-Jalil [2], Jorge Cantó [3,*], Damian Valdés-Santiago [4] and Laura Carballo-Sigler [1]

[1] Centro de Investigación en Ingeniería y Ciencias Aplicadas, Universidad Autónoma del Estado de Morelos, Ave. Universidad 1001, Chamilpa 62209, Mexico; eduardo.trutie@uaem.edu.mx (E.T.-C.); laura.carballo@uaem.edu.mx (L.C.-S.)
[2] Tecnologico de Monterrey, School of Engineering and Sciences, Reserva Territorial Atlixcáyotl, Puebla 72453, Mexico; jnietoj@tec.mx
[3] Corrosión y Protección (CyP), Buffon 46, Mexico City 11590, Mexico
[4] Facultad de Matemática y Computación, Universidad de La Habana, San Lázaro y L, Vedado, Plaza de la Revolución, La Habana 10400, Cuba; dvs89cs@matcom.uh.cu
* Correspondence: dseuret@uaem.mx (D.S.-J.); canto@corrosionyproteccion.com (J.C.)

Abstract: In this paper, we present six new contributions: two novel definitions and four groundbreaking theorems related to the theoretical foundations of the integral $\mathcal{T}_e$ transform, with a specific focus on analyzing functions with integrable modulus. The definitions referred to the $\mathcal{T}_e$ window and the $\mathcal{T}_e$ transform in two parameters, respectively. The theorems provide the main theoretical basis for the $\mathcal{T}_e$ transform: the existence of the $\mathcal{T}_e$ transform in two parameters, the $\mathcal{T}_e$ transform $\in L^1(\mathbb{R})$, the existence of the inverse $\mathcal{T}_e$ transform, and uniqueness of the $\mathcal{T}_e$ transform. These results reveal the importance of the fact that the $\mathcal{T}_e$ transform only depends on two parameters (translation and dyadic frequency), obtaining its inverse transformation more directly; hence, breaking through a new approach in function analysis by representing a function in the scale-frequency plane. The theoretical results presented in this paper are supported by the previous works of the authors.

Keywords: existence and uniqueness of $\mathcal{T}_e$ transform; inverse $\mathcal{T}_e$ transform; multi-sensitive spectrum; $\mathcal{T}_e$ transform; $\mathcal{T}_e$ window

MSC: 65T60; 42C40; 65F99; 65H10

check for updates

Citation: Trutié-Carrero, E.; Seuret-Jiménez, D.; Nieto-Jalil, J.M.; Cantó, J.; Valdés-Santiago, D.; Carballo-Sigler, L. The $\mathcal{T}_e$ Transform: A High-Resolution Integral Transform and Its Key Properties. *Mathematics* **2023**, *11*, 4495. https://doi.org/10.3390/math11214495

Academic Editor: Luís Castro

Received: 28 September 2023
Revised: 23 October 2023
Accepted: 25 October 2023
Published: 31 October 2023

Copyright: © 2023 by the authors. Licensee MDPI, Basel, Switzerland. This article is an open access article distributed under the terms and conditions of the Creative Commons Attribution (CC BY) license (https://creativecommons.org/licenses/by/4.0/).

1. Introduction

This paper presents six new contributions to the integral $\mathcal{T}_e$ transform in the field of mathematics applied to engineering.

The first contribution focuses on defining the $\mathcal{T}_e$ window, while the second contribution introduces the definition of the $\mathcal{T}_e$ transform in two parameters. The third contribution presents a theorem regarding the existence of the $\mathcal{T}_e$ transform, while the fourth establishes this transform belongs to $\in L^1(\mathbb{R})$. Furthermore, the fifth contribution demonstrates the existence of the inverse $\mathcal{T}_e$ transform, and lastly, the sixth contribution provides a uniqueness theorem for the $\mathcal{T}_e$ transform. The theoretical results presented in this paper were validated by the authors of the works shown in [1–4].

The problem of function recovery $(f(t),\ \forall\ t \in \mathbb{R})$ is very important in the field of applied mathematics [5–7]. In [2], the authors introduce the $\mathcal{T}_e$ transform, see Equation (1), as a dependent map of three parameters. This transform has as its main advantages the attenuation of the cross-terms and the isolation of the frequency components [2], which are achieved through the dyadic frequency spectrum. To have an integral transform dependent

on more than two parameters makes it difficult to represent them and obtaining their inverse integral transform becomes very difficult.

$$\mathcal{T}_e := \hat{f}_{DTe}[f(t)](\mu, \xi, \vartheta) = \int_{-\infty}^{\infty} f(t) w_\mu(t) \psi_{\xi,\mu}(t) e^{-i2\pi\vartheta t} dt, \tag{1}$$

where:

ϑ is the dyadic linear frequency [2],
t represents time or space, and
$w_\mu(t) = w(t-\mu), \forall \mu \in \mathbb{R}$ and $\psi_{\xi,\mu}(t) = \frac{1}{\sqrt{2^\xi}} \psi\left(\frac{t}{2^\xi} - \mu\right), \forall \xi \in \mathbb{Z}$ are the window function and the dyadic wavelet function, respectively.

While [2] presents a procedure for recovering a function $f(v)$, $\forall\ v \in \mathbb{R}$, where v represents either time or space, from its $\mathcal{T}_e$ transform, there is currently no theorem that provides a generalized equation for the recovery of $f(v)$.

Another challenge highlighted in Equation (1) is the presence of a function dependent on three parameters μ, ξ, ϑ. This complexity implies that obtaining its inverse integral transform may not be a straightforward process. Furthermore, additional issues arise, such as the lack of clarity regarding the existence and uniqueness of the $\mathcal{T}_e$ transform, as well as the functional space in which the $\mathcal{T}_e$ transform is defined. Therefore, this manuscript addresses these existing gaps.

The paper is organized as follows. Section 2 contains the theoretical background used in the proposed definitions and theorems. Section 3 shows the definitions and proposed theorems with their proofs. Section 4 shows the transformed pairs calculated by the $\mathcal{T}_e$ transform. Finally, the main conclusions are shown in Section 5.

2. Theoretical Background

This section provides the theoretical foundations used for analyzing a function $f(\upsilon)$ belonging to the subspace $L^1(\mathbb{R}) \cap L^2(\mathbb{R})$, which is dense in $L^2(\mathbb{R})$. These theoretical foundations will be employed in Section 3.

Fourier Transform and Its Inverse

The Fourier transform for a function $f(\upsilon)$ that is absolutely integrable is defined in Equation (2) and its inverse is defined in Equation (3) according to [8,9].

$$F(\omega) = \int_{-\infty}^{\infty} f(\upsilon) e^{-i\omega\upsilon} d\upsilon, \tag{2}$$

$$f(\upsilon) = \frac{1}{2\pi} \int_{-\infty}^{\infty} F(\omega) e^{i\omega v} d\omega, \tag{3}$$

where:

ω is the angular frequency,
υ represents time or space, and,
i is the complex unit.

- Parseval's Theorem [10–12], Equation (4), and Plancherel's Theorem [13–15] Equation (5), respectively

  If $f(\upsilon)$ and $h(\upsilon)$ are two functions on $L^1(\mathbb{R}) \cap L^2(\mathbb{R})$, then

$$\int_{-\infty}^{\infty} f(\upsilon) h^*(\upsilon) dt = \frac{1}{2\pi} \int_{-\infty}^{\infty} F(\omega) H^*(\omega) d\omega. \tag{4}$$

For $f(\upsilon) = h(\upsilon)$ it is obtained that

$$\int_{-\infty}^{\infty} |f(\upsilon)|^2 dt = \frac{1}{2\pi} \int_{-\infty}^{\infty} |F(\omega)|^2 d\omega, \tag{5}$$

where $F(\omega)$ is the Fourier transform $f(\upsilon)$, and $H^*(\omega)$ is the complex conjugate of the Fourier transform of $h(\upsilon)$.

- Fubini's Theorem [9,16,17]

If $\int_{-\infty}^{\infty}\left(\int_{-\infty}^{\infty} |f(\upsilon_1, \upsilon_2)| d\upsilon_1\right) d\upsilon_2 < +\infty$, then Equation (6) holds.

$$\int_{-\infty}^{\infty}\int_{-\infty}^{\infty} f(\upsilon_1, \upsilon_2) d\upsilon_1 d\upsilon_2 = \int_{-\infty}^{\infty}\left(\int_{-\infty}^{\infty} f(\upsilon_1, \upsilon_2) d\upsilon_1\right) d\upsilon_2 = \int_{-\infty}^{\infty}\left(\int_{-\infty}^{\infty} f(\upsilon_1, \upsilon_2) d\upsilon_2\right) d\upsilon_1 \tag{6}$$

where $f(\upsilon_1, \upsilon_2)$ represents an absolutely integrable function, permitting the interchangeability of the order of integration.

- Lebesgue's Dominated Convergence Theorem [18,19]

Let $\{f_n\}$ be a sequence of measurable functions on E that converges punctually to the function $f(\upsilon)$ and suppose that there exists an integrable function G on E such that $|f_n| \leq \mathrm{G}$, $\forall\, n \in N$, then

(a) $f(\upsilon)$ is integrable on E,
(b) $\int_E f(\upsilon) d\upsilon = \lim_{n\to\infty} \int_E f_n(\upsilon) d\upsilon$

- Function Composition Theorem [20,21]

Let $f(\upsilon)$ be an integrable function on the interval [A, B], and let $g(\upsilon)$ be a continuous function on the interval [E, Z]. Suppose that $f([\mathrm{A}, \mathrm{B}]) \subset g([\mathrm{E}, \mathrm{Z}])$. Then, $(g \circ f)(\upsilon)$ is integrable on [A, B] $\forall$ A, B, E, Z $\in \mathbb{R}$.

3. Results

This section presents the definitions, deduction, and theorems related to the $\mathcal{T}_e$ transform.

Definition 1 ($\mathcal{T}_e$ Window). *A bounded function $\beta_{\mu,\xi}(\upsilon)$, centered at $\upsilon = 0$, even, and in $L^1(\mathbb{R}) \cap L^2(\mathbb{R})$ is a $\mathcal{T}_e$ window; if it is the product of a bounded function $w_\mu(\upsilon)$ with $\|w_\mu\| = 1$ and a dyadic wavelet function, $\psi_{\mu,\xi}(\upsilon)$, where μ and ξ are the translation and scale parameters, respectively. Equation (7) shows the $\mathcal{T}_e$ window.*

$$\beta_{\mu,\xi}(\upsilon) = w_\mu(\upsilon) \cdot \psi_{\mu,\xi}(\upsilon), \tag{7}$$

where:
$\psi_{\mu,\xi}(\upsilon) = \frac{1}{\sqrt{2^\xi}} \psi\left(\frac{\upsilon}{2^\xi} - \mu\right) \in L^1(\mathbb{R}) \cap L^2(\mathbb{R})$, *and*
$w_\mu(\upsilon) = w(\upsilon - \mu) \in L^1(\mathbb{R}) \cap L^2(\mathbb{R})$.

In applied mathematics, it is necessary that the $\mathcal{T}_e$ window belongs to $L^1(\mathbb{R}) \cap L^2(\mathbb{R})$. This is because $L^2(\mathbb{R})$ is not a subspace of $L^1(\mathbb{R})$ [22]. Moreover, if $\beta_{\mu,\xi}(\upsilon) \in L^2(\mathbb{R})$ but $\beta_{\mu,\xi}(\upsilon) \notin L^1(\mathbb{R})$, then the Fourier transform of $\beta_{\mu,\xi}(\upsilon)$ cannot be computed by Equation (2) because $\beta_{\mu,\xi}(\upsilon)e^{-i\omega\upsilon}$ is not integrable [9], as per Lebesgue's theorem. This implies the need to bound our universe of functions to the set $L^1(\mathbb{R}) \cap L^2(\mathbb{R})$ dense in $L^2(\mathbb{R})$.

The significance of combining two window functions, as seen in Equation (7), one without the scale parameter, $w_\mu(\upsilon)$, and another with the scale parameter, $\psi_{\mu,\xi}(\upsilon)$, allows the possibility of discriminating spurious frequency components. The main goal of using

two windows with mentioned features is to find a plugin that maximizes the attenuation of unwanted frequency features.

Recently, the authors of [3,4] have utilized the $\mathcal{T}_e$ transform as a basis in hydraulic and seismic applications. They reported as the main innovation the $\mathcal{T}_e$ cross-spectral density, along with $\mathcal{T}_e$ coherence and the $\mathcal{T}_e$ gram, respectively. In their work, they achieved favorable results using a Daubechies 45 wavelet and a Kaiser-6 window. It is worth noting that the behavior of these windows is influenced by the parameter ξ, which, in turn, impacts the function $\beta_{\mu,\xi}(\upsilon)$. Consequently, the function $\beta_{\mu,\xi}(\upsilon)$ is also dependent on ξ.

Figure 1 shows an example for the previous discussion using a generic window function and a Daubechies 4 wavelet [23–25]. The effect explained earlier gives a redundancy effect that offers the possibility for maximizing the noise attenuation and cross-terms attenuation. Note that in Figure 1a–d, the gray region represents the area removed after multiplication. The results of the $\mathcal{T}_e$ window after contracting the dyadic wavelet function or the window function favor noise attenuation. This effect increases the sensitivity, obtaining a multi-sensitive spectrum.

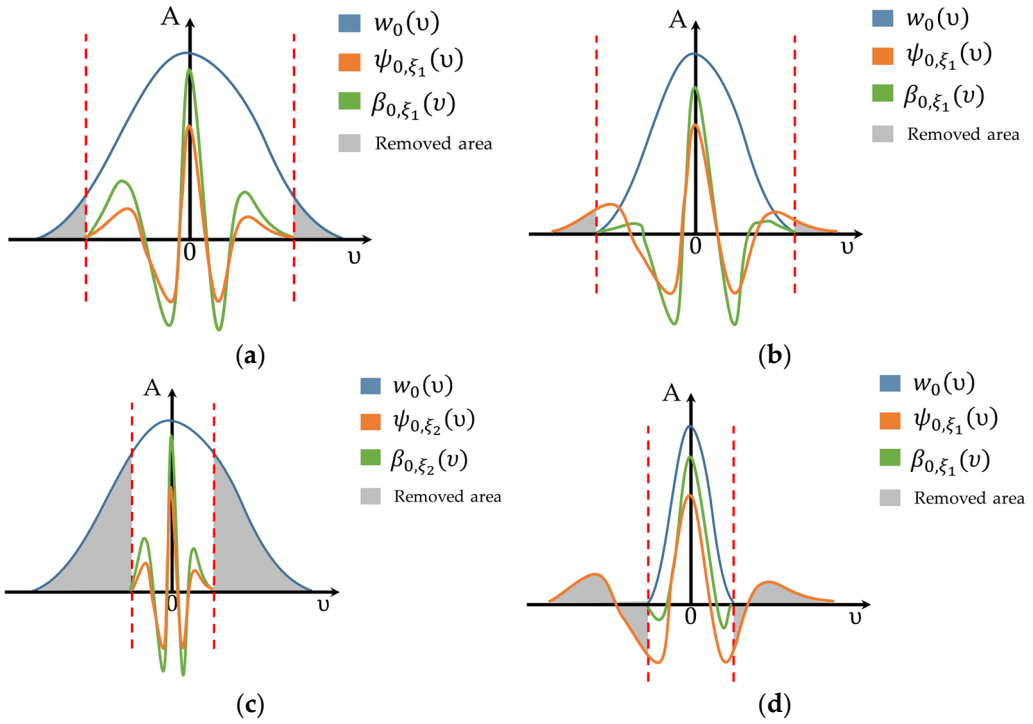

Figure 1. Relationship between two windows to obtain the $\mathcal{T}_e$ window. In (**a**,**c**), the dyadic wavelet is contracted. In (**b**,**d**), the window function is contracted.

Deduction 1 ($\mathcal{T}_e$ Transform in Two Parameters)**.** *We can rewrite Equation (1) as shown in Equation (8), considering the parameter of shift-invariance* $\mu = 0$ *[2], and at the scale* ξ_1.

$$\mathcal{T}_e[f(\upsilon)](\omega) = \frac{1}{\sqrt{2^{\xi_1}}} \int_{-\infty}^{\infty} f(\upsilon)\beta_{0,\xi_1}(\upsilon)e^{-i\omega\upsilon}d\upsilon, \tag{8}$$

$$\mathcal{T}_e[f(\upsilon)](\omega) = \frac{1}{\sqrt{2^{\xi_1}}} \int_{-\infty}^{\infty} f(\upsilon)\beta_0\left(\frac{\upsilon}{2^{\xi_1}}\right)e^{-i\omega\upsilon}d\upsilon. \tag{9}$$

If we make a change of parameters, in Equation (9), $\frac{v}{2^{\xi_1}} = \tau$ *obtaining that* $dv = 2^{\xi_1} d\tau$*, we realize that* $\beta_0\left(\frac{v}{2^{\xi}}\right)$ *is bounded and is multiplying the function* $f(v)$*. Then, by Figure 2, we rewrite Equation (9) as shown in Equation (10).*

$$\mathcal{T}_e[f(v)]\left(2^{\xi_1}\omega\right) = \frac{1}{\sqrt{2^{\xi_1}}}\int_a^b h(\tau)e^{-i\omega 2^{\xi_1}\tau}2^{\xi_1}d\tau. \tag{10}$$

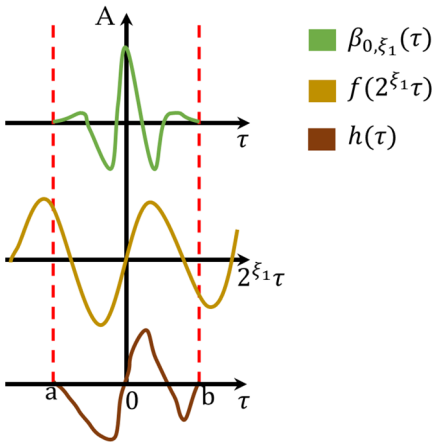

Figure 2. Result obtained after multiplying the $\mathcal{T}_e$ window and the function to be analyzed, resulting in $h(\tau)$.

If we compare Equation (10) with Equation (2), we can observe that we are in the presence of the Fourier transform of $h(\tau)$*. After rearranging Equation (10), we obtain Equation (11).*

$$\mathcal{T}_e[h(\tau)]\left(2^{\xi_1}\omega\right) = \sqrt{2^{\xi_1}}H\left(2^{\xi_1}\omega\right). \tag{11}$$

This result indicates how the frequency domain is scaled. If we consider the translation parameter, then we can express the result of Equation (11) as $\mathcal{T}_e[f(v)](\mu, 2^{\xi}\omega)$ *due to the shift-invariance property [2]. This indicates the possibility of expressing Equation (1) in two parameters, making way to Definition 2.*

Expressing the $\mathcal{T}_e$ transform in two parameters allows us to interpret the two-dimensional behavior of the $\mathcal{T}_e$ spectrum for a function $f(v)$. From the point of view of applied mathematics, the $\mathcal{T}_e$ transform continues to provide localized information in dyadic time-frequency. Only when compacting its output information is it observed how the frequency is scaled by a dyadic factor. Previous research conducted by the authors of this paper demonstrates that such scaling enables the isolation of frequency components, the attenuation of cross-terms, and the identification of system behaviors [1–4].

Theorem 1 (Existence of the $\mathcal{T}_e$ Transform in Two Parameters)**.** *Let Equation (12) be the* $\mathcal{T}_e$ *transform for a function* $f(v)$*, it will be shown below that there exists the* $\mathcal{T}_e$ *transform in two parameters.*

$$\mathcal{T}_e[f(v)](\mu, 2^{\xi}\omega) = \int_{-\infty}^{\infty} f(v)\beta_{\mu,\xi}(v)e^{-i\omega v}dv. \tag{12}$$

If $f(v)$ *and* $\beta_{\mu,\xi}(v) \in L^1(\mathbb{R}) \cap L^2(\mathbb{R})$*, then* $\exists\ \mathcal{T}_e[f(v)](\mu, 2^{\xi}\omega)$.

Proof. To carry out the demonstration, we will calculate the integral of the module of the integrand of Equation (12). This is

$$\int_{-\infty}^{\infty} \left| f(\upsilon)\beta_{\mu,\xi}(\upsilon)e^{-i\omega\upsilon} \right| d\upsilon = \int_{-\infty}^{\infty} \left| f(\upsilon)\beta_{\mu,\xi}(\upsilon) \right| \left| e^{-i\omega\upsilon} \right| d\upsilon.$$

Since $f(v)$ and $\beta_{\mu,\xi}(v)$ are in $L^1(\mathbb{R}) \cap L^2(\mathbb{R})$, then $f(v)\beta_{\mu,\xi}(v)$ is in $L^1(\mathbb{R}) \cap L^2(\mathbb{R})$ which means $\left| f(v)\beta_{\mu,\xi}(v) \right|$ is absolutely integrable. Also, $\left| e^{-i\omega v} \right| = 1$. Then, Equation (13) is fulfilled proving that the $\mathcal{T}_e$ transform of $f(v)$ exists.

$$\int_{-\infty}^{\infty} |f(\upsilon)| \left| \beta_{\mu,\xi}(\upsilon) \right| \left| e^{-i\omega\upsilon} \right| d\upsilon = \int_{-\infty}^{\infty} \left| f(\upsilon)\beta_{\mu,\xi}(\upsilon) \right| d\upsilon < \infty. \tag{13}$$

□

This theorem is fundamental in the field of signal analysis and system theory. Because it states that a function that is in $L^1(\mathbb{R}) \cap L^2(\mathbb{R})$, its frequency spectrum is decomposed dyadically, obtaining different combinations of sinusoidal frequencies, which is essential for the analysis of the frequency components of a function.

Definition 2 ($\mathcal{T}_e$ Transform in Two Parameters)**.** *Given $f(v) \in L^1(\mathbb{R}) \cap L^2(\mathbb{R})$, the $\mathcal{T}_e$ transform in two parameters of $f(v)$ is defined as shown in Equation (12).*

Theorem 2 ($\mathcal{T}_e$ Transform $\in L^1(\mathbb{R})$)**.** *If $f(v) \in L^1(\mathbb{R})$, then $\mathcal{T}_e[f(v)] \in L^1(\mathbb{R})$.*

Proof. To carry out the demonstration, it is enough to prove that $\mathcal{T}_e[f(v)]\left(\mu, 2^{\xi}\omega\right)$ converges punctually. To do this, we are going to use Lebesgue's dominated convergence theorem, shown in Section 2. For this, we calculate the $\mathcal{T}_e$ transform of $f(v)$ around the angular frequency χ, as shown in Equation (14).

$$\mathcal{T}_{\mathrm{e}}[f(\upsilon)]\left(\mu, 2^{\xi}\{\omega+\chi\}\right) - \mathcal{T}_{\mathrm{e}}[f(\upsilon)]\left(\mu, 2^{\xi}\omega\right) = \int_{-\infty}^{\infty} f(\upsilon)\beta_{\mu,\xi}(\upsilon)\left[e^{-i(\omega+\chi)\upsilon} - e^{-i\omega\upsilon}\right] d\upsilon. \tag{14}$$

Rearranging the integrand, we obtain Equation (15).

$$\int_{-\infty}^{\infty} f_{\chi}(\upsilon) d\upsilon = \int_{-\infty}^{\infty} f(\upsilon)\beta_{\mu,\xi}(\upsilon)e^{-i\omega\upsilon}\left[e^{-i\chi\upsilon} - 1\right] d\upsilon, \tag{15}$$

where $f_{\chi}(v) = f(v)\beta_{\mu,\xi}(v)e^{-i\omega v}\left[e^{-i\chi v} - 1\right]$. Subsequently, $\lim_{\chi\to 0} f_{\chi}(v)$ is calculated, see Equation (16).

$$\lim_{\chi\to 0} f_{\chi}(\upsilon) = f(\upsilon)\beta_{\mu,\xi}(\upsilon)e^{-i\omega\upsilon} \lim_{\chi\to 0}\left(e^{-i\chi\upsilon} - 1\right) = 0. \tag{16}$$

After calculating $\lim_{\chi\to 0} f_{\chi}(v)$ and because $|f(v)|$ is integrable using the dominated convergence theorem, we obtain that $\mathcal{T}_e[f(v)]\left(\mu, 2^{\xi}\omega\right) \in L^1(\mathbb{R})$. □

The main importance of having the $\mathcal{T}_e$ transform in $L^1(\mathbb{R})$ is that it allows analyzing functions in terms of their spectral content, revealing what the composition of the function is like in the dyadic frequency domain to then be able to recover said function.

Theorem 3 (Existence of the Inverse $\mathcal{T}_e$ Transform). *If $f(v) \in L^1(\mathbb{R}) \cap L^2(\mathbb{R})$, then Equation (17) is the inverse $\mathcal{T}_e$ transform.*

$$f(v) = \frac{1}{2\pi} \int_{-\infty}^{\infty} \int_{-\infty}^{\infty} \mathcal{T}_e[f(v)]\left(\mu, 2^{\xi}\omega\right) \beta_{\mu,\xi}(v) e^{i\omega v} d\omega d\mu. \tag{17}$$

Proof. To perform the proof, we first calculate the Fourier transform of $\mathcal{T}_e[f(v)]\left(\mu, 2^{\xi}\omega\right)$ for μ.

$$\mathcal{F}\left\{\mathcal{T}_e[f(\upsilon)]\left(\mu, 2^{\xi}\omega\right)\right\} = \int_{-\infty}^{\infty} \int_{-\infty}^{\infty} f(\upsilon)\beta_{\mu,\xi}(\upsilon) e^{-i\omega\upsilon} d\upsilon e^{-i\chi\mu} d\mu, \tag{18}$$

where:

χ is the angular frequency associated with μ,
$\mathcal{F}$ represents the operator of the Fourier transform, and we will use this notation whenever we depict the Fourier transform of the $\mathcal{T}_e$ transform.

Applying Fubini's theorem, we obtain Equation (19).

$$\mathcal{F}\left\{\mathcal{T}_e[f(\upsilon)]\left(\mu, 2^{\xi}\omega\right)\right\} = \int_{-\infty}^{\infty} f(\upsilon) e^{-i\omega\upsilon} \int_{-\infty}^{\infty} \beta_{\mu,\xi}(\upsilon) e^{-i\chi\mu} d\mu \, d\upsilon. \tag{19}$$

Since the $\mathcal{T}_e$ window is even and holds the scaling property of a dyadic wavelet function, the Fourier transform of $\beta_{\mu,\xi}(v)$ associated with μ is calculated as follows:

$$B(v,\chi) = \frac{1}{\sqrt{2^{\xi}}} \int_{-\infty}^{\infty} \beta\left(\mu - \frac{v}{2^{\xi}}\right) e^{-i\chi\mu} d\mu.$$

We make a change of variable $\mu - \frac{v}{2^{\xi}} = \tau$, obtaining $\mu = \tau + \frac{v}{2^{\xi}}$ and $d\mu = d\tau$:

$$B(v,\chi) = \frac{1}{\sqrt{2^{\xi}}} e^{-i\chi\frac{v}{2^{\xi}}} \int_{-\infty}^{\infty} \beta(\tau) e^{-i\chi\tau} d\tau,$$

$$B(v,\chi) = \frac{1}{\sqrt{2^{\xi}}} e^{-i\chi\frac{v}{2^{\xi}}} B(\chi). \tag{20}$$

If we use the result obtained in Equation (20) in Equation (19), we obtain Equation (21). Those steps are shown below.

$$\mathcal{F}\left\{\mathcal{T}_e[f(v)]\left(\mu, 2^{\xi}\omega\right)\right\} = \int_{-\infty}^{\infty} f(v) \frac{1}{\sqrt{2^{\xi}}} e^{-i\chi\frac{v}{2^{\xi}}} B(\chi) e^{-i\omega v} dv,$$

$$\mathcal{F}\left\{\mathcal{T}_e[f(v)]\left(\mu, 2^{\xi}\omega\right)\right\} = \frac{1}{\sqrt{2^{\xi}}} \int_{-\infty}^{\infty} f(v) B(\chi) e^{-i[\omega + \frac{\chi}{2^{\xi}}]v} dv,$$

$$\mathcal{F}\left\{\mathcal{T}_e[f(v)]\left(\mu, 2^{\xi}\omega\right)\right\} = \frac{1}{\sqrt{2^{\xi}}} B(\chi) \int_{-\infty}^{\infty} f(v) e^{-i[\omega + \frac{\chi}{2^{\xi}}]v} dv,$$

$$\mathcal{F}\left\{\mathcal{T}_e[f(\upsilon)]\left(\mu, 2^{\xi}\omega\right)\right\} = \frac{1}{\sqrt{2^{\xi}}} \mathrm{B}(\chi) \mathcal{F}[f(\upsilon)]\left(\omega + \frac{\chi}{2^{\xi}}\right). \tag{21}$$

Then, we apply Parseval's theorem to the integral that is between the square brackets, obtaining Equation (23).

$$f(\upsilon) = \frac{1}{2\pi}\int_{-\infty}^{\infty}\left[\int_{-\infty}^{\infty}\mathcal{T}_e[f(\upsilon)]\left(\mu, 2^{\xi}\omega\right)\beta_{\mu,\xi}(\upsilon)d\mu\right]e^{i\omega\upsilon}d\omega, \tag{22}$$

$$f(\upsilon) = \frac{1}{2\pi}\int_{-\infty}^{\infty}\left[\frac{1}{2\pi}\int_{-\infty}^{\infty}\frac{1}{\sqrt{2^{\xi}}}\mathrm{B}(\chi)\mathcal{F}[f(\upsilon)]\left(\omega+\frac{\chi}{2^{\xi}}\right)\left[\frac{1}{\sqrt{2^{\xi}}}e^{-i\chi\frac{\upsilon}{2^{\xi}}}\mathrm{B}(\chi)\right]^{*}d\chi\right]e^{i\omega\upsilon}d\omega, \tag{23}$$

where * is the complex conjugate operator.

Rewriting Equation (23), we obtain Equation (24).

$$f(\upsilon) = \frac{1}{2\pi}\int_{-\infty}^{\infty}\left[\frac{1}{2\pi}\int_{-\infty}^{\infty}\mathrm{F}\left(\omega+\frac{\chi}{2^{\xi}}\right)\frac{1}{\sqrt{2^{\xi}}}\mathrm{B}(\chi)\frac{1}{\sqrt{2^{\xi}}}\mathrm{B}^{*}(\chi)e^{i\chi\frac{\upsilon}{2^{\xi}}}d\chi\right]e^{i\omega\upsilon}d\omega. \tag{24}$$

Since $\frac{1}{\sqrt{2^{\xi}}} \in \mathbb{R}$, this means that $\frac{1}{\sqrt{2^{\xi}}}B(\chi)\frac{1}{\sqrt{2^{\xi}}}B^{*}(\chi)$ can be rewritten as $\left|B^{'}(\chi)\right|^{2}$.

Rewriting Equation (24) and applying Fubini's theorem (see Section 2), we obtain Equation (25).

$$f(\upsilon) = \left(\frac{1}{2\pi}\right)^{2}\int_{-\infty}^{\infty}\int_{-\infty}^{\infty}\mathrm{F}\left(\omega+\frac{\chi}{2^{\xi}}\right)\left|\mathrm{B}'(\chi)\right|^{2}e^{i[\omega+\frac{\chi}{2^{\xi}}]\upsilon}d\omega d\chi \tag{25}$$

Then, we organize the integral of Equation (25) to express it as observed in Equation (26).

$$f(\upsilon) = \frac{1}{2\pi}\int_{-\infty}^{\infty}\left[\frac{1}{2\pi}\int_{-\infty}^{\infty}\mathrm{F}\left(\omega+\frac{\chi}{2^{\xi}}\right)e^{i(\omega+2^{-\xi}\chi)\upsilon}d\omega\right]\left|\mathrm{B}'(\chi)\right|^{2}d\chi \tag{26}$$

To solve Equation (26), we first make a change of variable to the integral inside the square brackets $\omega^{'} = \omega + 2^{-\xi}\chi$ and $d\omega' = d\omega + d\left(2^{-\xi}\chi\right)$ obtaining $d\omega' = d\omega$. Equation (27) shows this integral with the change of variables. Observe that we are in the presence of the inverse Fourier transform of the function $F(\omega')$, obtaining $f(\upsilon)$.

$$f(\upsilon) = \frac{1}{2\pi}\int_{-\infty}^{\infty}F\left(\omega'\right)e^{i\omega'\upsilon}d\omega'. \tag{27}$$

If we substitute the result of Equation (27) in Equation (26), we obtain Equation (28).

$$f(\upsilon) = \frac{1}{2\pi}\int_{-\infty}^{\infty}f(\upsilon)\left|\mathrm{B}'(\chi)\right|^{2}d\chi. \tag{28}$$

Then, we rewrite Equation (28) obtaining Equation (29),

$$f(\upsilon) = \frac{f(\upsilon)}{2\pi}\int_{-\infty}^{\infty}\left|\mathrm{B}'(\chi)\right|^{2}d\chi. \tag{29}$$

Through reference [9] and applying Plancherel's theorem, we obtain Equation (30).

$$\int_{-\infty}^{\infty}\left|\beta_{\mu,\xi}(\upsilon)\right|^{2}d\mu = \frac{1}{2\pi}\int_{-\infty}^{\infty}\left|B^{'}(\chi)\right|^{2}d\chi = 1. \tag{30}$$

Then, the identity $f(v) = f(v)$ holds, which indicates that the inverse $\mathcal{T}_e$ transform exists. □

Having a tool that allows us to recover a function from the dyadic frequency domain is highly valuable in system analysis. This is because it simplifies function analysis through dyadic frequency representation, particularly when dealing with complex or noisy functions. Additionally, it enables noise reduction by isolating and eliminating unwanted or spurious frequency components.

Theorem 4 (Uniqueness)**.** *Let $f : \mathbb{R} \to \mathbb{R}$ and $g : \mathbb{R} \to \mathbb{R}$ be two functions for which there are their $\mathcal{T}_e$ transforms. Then, $\mathcal{T}_e[f(v)]\left(\mu, 2^{\xi}\omega\right) = \mathcal{T}_e[g(v)]\left(\mu, 2^{\xi}\omega\right)$ if and only if $f(v) = g(v)$ almost everywhere.*

Proof. Necessity: To carry out the demonstration, we first calculate the magnitude of the difference of the $\mathcal{T}_e$ transform for $f(v)$ and $g(v)$. Finally, we use Theorem 3 (Existence of the inverse $\mathcal{T}_e$ transform) to use the inverse $\mathcal{T}_e$ transform.

$$|\mathcal{T}_e[f(\upsilon)] - \mathcal{T}_e[g(\upsilon)]|\left(\mu, 2^{\xi}\omega\right) = \left|\int_{-\infty}^{\infty} f(\upsilon)\beta_{\mu,\xi}(\upsilon)e^{-i\omega\upsilon}d\upsilon - \int_{-\infty}^{\infty} g(\upsilon)\beta_{\mu,\xi}(\upsilon)e^{-i\omega\upsilon}d\upsilon\right|,$$

$$\left|\int_{-\infty}^{\infty} [f(\upsilon) - g(\upsilon)]\beta_{\mu,\xi}(\upsilon)e^{-i\omega\upsilon}d\upsilon\right| \leq \int_{-\infty}^{\infty} |f(\upsilon) - g(\upsilon)||\beta_{\mu,\xi}(\upsilon)|\left|e^{-i\omega\upsilon}\right|d\upsilon.$$

Since $\left|e^{-i\omega\upsilon}\right| = 1$, then

$$\left|\int_{-\infty}^{\infty} [f(\upsilon) - g(\upsilon)]\beta_{\mu,\xi}(\upsilon)e^{-i\omega\upsilon}d\upsilon\right| \leq \int_{-\infty}^{\infty} |f(\upsilon) - g(\upsilon)||\beta_{\mu,\xi}(\upsilon)|d\upsilon = 0.$$

Sufficiency: To prove the other sense of equivalence, we will use the shown linearity property [2] for the $\mathcal{T}_e$ transform and the inverse $\mathcal{T}_e$ transform theorem shown in Theorem 3:

$$f(v) - g(v) = \frac{1}{2\pi}\int_{-\infty}^{\infty}\int_{-\infty}^{\infty} \mathcal{T}_e[f(v) - g(v)]\left(\mu, 2^{\xi}\omega\right)\beta_{\mu,\xi}(v)e^{i\omega v}d\omega d\mu = 0.$$

Since $\mathcal{T}_e[f(v) - g(v)]\left(\mu, 2^{\xi}\omega\right) = \int_{-\infty}^{\infty} f(v)\beta_{\mu,\xi}(v)e^{-i\omega v}dv - \int_{-\infty}^{\infty} g(v)\beta_{\mu,\xi}(v)e^{-i\omega v}dv = 0$. □

The uniqueness theorem in the $\mathcal{T}_e$ transform is a fundamental property that states that a function in the time domain is completely determined by its $\mathcal{T}_e$ transform in the dyadic frequency domain. From an applied mathematics point of view, such a theorem guarantees that, given the dyadic frequency spectrum of a function, it is possible to recover the original function in the time domain in a unique way. This is crucial in applications where functions need to be reconstructed from their spectrum, such as in communication, signal processing, and data retrieval.

4. Examples of Transformed Pairs

- **$\mathcal{T}_e$ Transform of the constant $f(\omega_c\upsilon)$ where $\omega_c = 0$:**

$$\mathcal{T}_e[f(0)]\left(\mu, 2^{\xi}\omega\right) = \int_{-\infty}^{\infty} f(0)\beta_{\mu,\xi}(\upsilon)e^{-i\omega\upsilon}d\upsilon,$$

$$\mathcal{T}_e[f(0)]\left(\mu, 2^{\xi}\omega\right) = f(0)\frac{1}{\sqrt{2^{\xi}}}\int_{-\infty}^{\infty}\beta\left(\frac{\upsilon}{2^{\xi}} - \mu\right)e^{-i\omega\upsilon}d\upsilon.$$

We make a change of variable $\frac{\upsilon}{2^{\xi}} - \mu = \tau$, obtaining $\upsilon = 2^{\xi}(\tau + \mu)$ and $d\upsilon = 2^{\xi}d\tau$,

$$\mathcal{T}_e[f(0)]\left(\mu, 2^{\xi}\omega\right) = 2^{\xi}f(0)\frac{1}{\sqrt{2^{\xi}}}\int_{-\infty}^{\infty}\beta(\tau)e^{-i\omega 2^{\xi}(\tau+\mu)}d\tau,$$

$$\mathcal{T}_e[f(0)]\left(\mu, 2^{\xi}\omega\right) = f(0)\sqrt{2^{\xi}}e^{-i\omega 2^{\xi}\mu}\int_{-\infty}^{\infty}\beta(\tau)e^{-i\omega 2^{\xi}\tau}d\tau,$$

$$\mathcal{T}_e[f(0)]\left(\mu, 2^{\xi}\omega\right) = f(0)\sqrt{2^{\xi}}e^{-i\omega 2^{\xi}\mu}\mathrm{B}\left(2^{\xi}\omega\right).$$

where $f(0)$ is a constant and $\mathrm{B}\left(2^{\xi}\omega\right)$ is the dyadic frequency response of $\beta(\tau)$ for $\omega_c = 0$ and it is the angular center frequency.

Figure 3 shows the frequency spectrum obtained for the $\mathcal{T}_e$ transform of the function $f(0)$. Note in this figure that there is a frequency spectrum for each value of ξ, obtaining a $\mathcal{T}_e$ window for each scale (2^{ξ} where $\xi \in [1\ 3]$). The authors call this result a dyadic frequency spectrum because ω is dilated by a factor of 2^{ξ}.

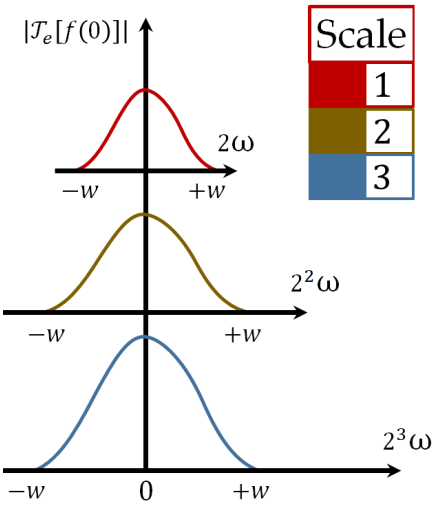

Figure 3. Dyadic frequency spectrum for $f(0)$, where w is the width of the $\mathcal{T}_e$ window and 2^{ξ} is the scale.

- **$\mathcal{T}_e$ Transform of the complex exponential:**

$$\mathcal{T}_e\left[e^{i\omega_c\upsilon}\right]\left(\mu, 2^{\xi}\omega\right) = \frac{1}{\sqrt{2^{\xi}}}\int_{-\infty}^{\infty}e^{i\omega_c\upsilon}\beta_{\mu,\xi}(\upsilon)e^{-i\omega\upsilon}d\upsilon,$$

$$\mathcal{T}_e\left[e^{i\omega_c\upsilon}\right]\left(\mu, 2^{\xi}\omega\right) = \frac{1}{\sqrt{2^{\xi}}}\int_{-\infty}^{\infty}\beta\left(\frac{\upsilon}{2^{\xi}} - \mu\right)e^{-i(\omega-\omega_c)\upsilon}d\upsilon.$$

We make a change of variable $\frac{\upsilon}{2^{\xi}} - \mu = \tau$, obtaining $\upsilon = 2^{\xi}(\tau + \mu)$ and $d\upsilon = 2^{\xi}d\tau$,

$$\mathcal{T}_e\left[e^{-i\omega_c\upsilon}\right]\left(\mu, 2^{\xi}\omega\right) = \sqrt{2^{\xi}}\int_{-\infty}^{\infty}\beta(\tau)e^{-i(\omega-\omega_c)2^{\xi}(\tau+\mu)}d\tau,$$

$$\mathcal{T}_e\left[e^{i\omega_c\upsilon}\right]\left(\mu,2^{\xi}\omega\right)=\sqrt{2^{\xi}}e^{-i(\omega-\omega_c)2^{\xi}\mu}\int_{-\infty}^{\infty}\beta(\tau)e^{-i(\omega-\omega_c)2^{\xi}\tau}d\tau,$$

$$\mathcal{T}_e\left[e^{i\omega_c\upsilon}\right]\left(\mu,2^{\xi}\omega\right)=\sqrt{2^{\xi}}e^{-i(\omega-\omega_c)2^{\xi}\mu}\mathrm{B}\left(2^{\xi}[\omega-\omega_c]\right).$$

Figure 4 shows the dyadic frequency spectrum obtained after calculating the $\mathcal{T}_e$ transform to the function $e^{i\omega_c\upsilon}$. Note that the frequency spectrum does not distort the frequency component, showing how it can be observed at different scales. For this case, we can see how if we multiply the $\mathcal{T}_e$ window by $e^{i\omega_c\upsilon}$, we obtain a translation of the window for ω_c. Furthermore, since the window has a limited spectral bandwidth, we can observe how this bandwidth is modified by the scale, showing the existence of different bandwidths that indicate sensitive behavior for different frequency components, known as multi-sensitivity.

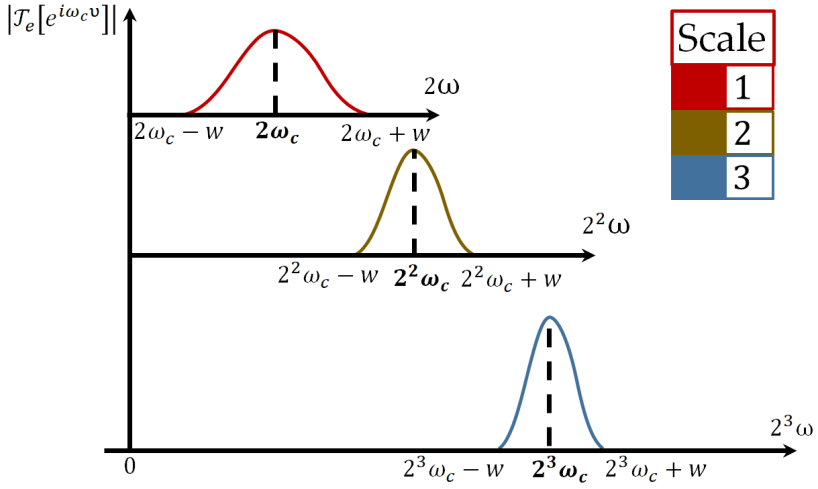

Figure 4. Dyadic frequency spectrum for $e^{i\omega_c\upsilon}$.

- **$\mathcal{T}_e$ Transform of the sine function:**

$$\mathcal{T}_e[\sin(\omega_c\upsilon)]\left(\mu,2^{\xi}\omega\right)=\int_{-\infty}^{\infty}\sin(\omega_c\upsilon)\beta_{\mu,\xi}(\upsilon)e^{-i\omega\upsilon}d\upsilon,$$

$$\mathcal{T}_e\left[\frac{e^{i\omega_c\upsilon}-e^{-i\omega_c\upsilon}}{2i}\right]\left(\mu,2^{\xi}\omega\right)=\frac{1}{\sqrt{2^{\xi}}2i}\left[\int_{-\infty}^{\infty}e^{i\omega_c\upsilon}\beta\left(\frac{\upsilon}{2^{\xi}}-\mu\right)e^{-i\omega\upsilon}d\upsilon-\int_{-\infty}^{\infty}e^{-i\omega_c\upsilon}\beta\left(\frac{\upsilon}{2^{\xi}}-\mu\right)e^{-i\omega\upsilon}d\upsilon\right],$$

$$\mathcal{T}_e\left[\frac{e^{i\omega_c\upsilon}-e^{-i\omega_c\upsilon}}{2i}\right]\left(\mu,2^{\xi}\omega\right)=\frac{1}{\sqrt{2^{\xi}}2i}\left[\int_{-\infty}^{\infty}\beta\left(\frac{\upsilon}{2^{\xi}}-\mu\right)e^{-i(\omega-\omega_c)\upsilon}d\upsilon-\int_{-\infty}^{\infty}\beta\left(\frac{\upsilon}{2^{\xi}}-\mu\right)e^{-i(\omega+\omega_c)\upsilon}d\upsilon\right],$$

We make a change of variable $\frac{\upsilon}{2^{\xi}}-\mu=\tau$, obtaining $\upsilon=2^{\xi}(\tau+\mu)$ and $d\upsilon=2^{\xi}d\tau$,

$$\mathcal{T}_e\left[\frac{e^{i\omega_c\upsilon}-e^{-i\omega_c\upsilon}}{2i}\right]\left(\mu,2^{\xi}\omega\right)=\frac{2^{\xi}}{\sqrt{2^{\xi}}2i}\left[\int_{-\infty}^{\infty}\beta(\tau)e^{-i(\omega-\omega_c)2^{\xi}(\tau+\mu)}d\tau-\int_{-\infty}^{\infty}\beta(\tau)e^{-i(\omega+\omega_c)2^{\xi}(\tau+\mu)}d\tau\right],$$

$$\mathcal{T}_e\left[\frac{e^{i\omega_c\upsilon}-e^{-i\omega_c\upsilon}}{2i}\right]\left(\mu,2^{\xi}\omega\right)=\frac{\sqrt{2^{\xi}}}{2i}\left[e^{-i(\omega-\omega_c)2^{\xi}\mu}\int_{-\infty}^{\infty}\beta(\tau)e^{-i(\omega-\omega_c)2^{\xi}\tau}d\tau-e^{-i(\omega+\omega_c)2^{\xi}\mu}\int_{-\infty}^{\infty}\beta(\tau)e^{-i(\omega+\omega_c)2^{\xi}\tau}d\tau\right],$$

$$\mathcal{T}_e[\sin(\omega_c \upsilon)]\left(\mu, 2^{\xi}\omega\right) = i\sqrt{2^{\xi-2}}\left[-e^{-i(\omega-\omega_c)2^{\xi}\mu}\mathrm{B}\left(2^{\xi}[\omega-\omega_c]\right) + e^{-i(\omega+\omega_c)2^{\xi}\mu}\mathrm{B}\left(2^{\xi}[\omega+\omega_c]\right)\right].$$

Figure 5 shows the $\mathcal{T}_e$ transform of the sine function. Notice how the result obtained is similar to that of the Fourier transform of a sine function [26–28]. This is because the $\mathcal{T}_e$ transform is derived from the Fourier transform. For this reason, we observe how we have a bilateral and odd spectrum. An evident advantage of the $\mathcal{T}_e$ transform over the Fourier transform and even the short-time Fourier transform [29,30] is the possibility of dyadic scaling of the frequency spectrum of the sine function. This allows a dyadic representation of said function to be obtained.

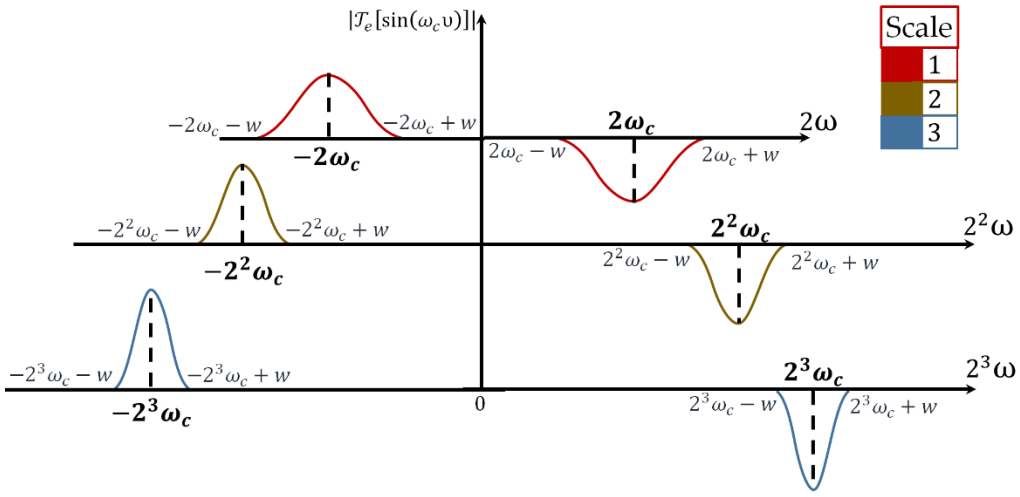

Figure 5. Dyadic frequency spectrum for $sin(\omega_c \upsilon)$.

This example reveals how the dyadic frequency spectrum preserves the bilateral frequency spectrum, now called the bilateral dyadic frequency spectrum. The fact of having a window function that contracts in the frequency domain will allow discriminating frequency components over ω_c.

- **$\mathcal{T}_e$ Transform of the cosine function:**

Notice how in this example a very similar result to the one obtained for the $\mathcal{T}_e$ transform of the sine function is obtained.

$$\mathcal{T}_e[\cos(\omega_c \upsilon)]\left(\mu, 2^{\xi}\omega\right) = \int_{-\infty}^{\infty} \cos(\omega_c \upsilon)\beta_{\mu,\xi}(\upsilon)e^{-i\omega\upsilon}d\upsilon,$$

$$\mathcal{T}_e\left[\frac{e^{i\omega_c\upsilon}+e^{-i\omega_c\upsilon}}{2}\right]\left(\mu, 2^{\xi}\omega\right) = \frac{1}{\sqrt{2^{\xi}2}}\left[\int_{-\infty}^{\infty} e^{i\omega_c\upsilon}\beta\left(\frac{\upsilon}{2^{\xi}}-\mu\right)e^{-i\omega\upsilon}d\upsilon + \int_{-\infty}^{\infty} e^{-i\omega_c\upsilon}\beta\left(\frac{\upsilon}{2^{\xi}}-\mu\right)e^{-i\omega\upsilon}d\upsilon\right],$$

$$\mathcal{T}_e\left[\frac{e^{i\omega_c\upsilon}+e^{-i\omega_c\upsilon}}{2}\right]\left(\mu, 2^{\xi}\omega\right) = \frac{\sqrt{2^{\xi}}}{2^{\xi}2}\left[\int_{-\infty}^{\infty} \beta\left(\frac{\upsilon}{2^{\xi}}-\mu\right)e^{-i(\omega-\omega_c)\upsilon}d\upsilon + \int_{-\infty}^{\infty} \beta\left(\frac{\upsilon}{2^{\xi}}-\mu\right)e^{-i(\omega+\omega_c)\upsilon}d\upsilon\right].$$

We make a change of variables $\frac{\upsilon}{2^{\xi}} - \mu = \tau$, obtaining $\upsilon = 2^{\xi}(\tau+\mu)$ and $d\upsilon = 2^{\xi}d\tau$,

$$\mathcal{T}_e\left[\frac{e^{i\omega_c\upsilon}+e^{-i\omega_c\upsilon}}{2}\right]\left(\mu, 2^{\xi}\omega\right) = \frac{\sqrt{2^{\xi}}}{2^{\xi}2}2^{\xi}\left[\int_{-\infty}^{\infty} \beta(\tau)e^{-i(\omega-\omega_c)2^{\xi}(\tau+\mu)}d\tau + \int_{-\infty}^{\infty} \beta(\tau)e^{-i(\omega+\omega_c)2^{\xi}(\tau+\mu)}d\tau\right],$$

$$\mathcal{T}_e[\cos(\omega_c \upsilon)]\left(\mu, 2^{\xi}\omega\right) = \sqrt{2^{\xi-2}}\left[e^{-i(\omega-\omega_c)2^{\xi}\mu}\int_{-\infty}^{\infty} \beta(\tau)e^{-i(\omega-\omega_c)2^{\xi}\tau}d\tau + e^{-i(\omega+\omega_c)2^{\xi}\mu}\int_{-\infty}^{\infty} \beta(\tau)e^{-i(\omega+\omega_c)2^{\xi}\tau}d\tau\right],$$

$$\mathcal{T}_e[\cos(\omega_c v)]\left(\mu, 2^{\xi}\omega\right) = \sqrt{2^{\xi-2}}\left[e^{-i(\omega-\omega_c)2^{\xi}\mu}\mathrm{B}\left(2^{\xi}[\omega-\omega_c]\right) + e^{-i(\omega+\omega_c)2^{\xi}\mu}\mathrm{B}\left(2^{\xi}[\omega+\omega_c]\right)\right].$$

Figure 6 shows the dyadic frequency spectrum for a cosine function. It is worth noting how this frequency spectrum retains the parity characteristic observed in the frequency spectrum obtained through the Fourier transform [28,31], adding the advantage of being able to analyze the frequency component of the function in different scales.

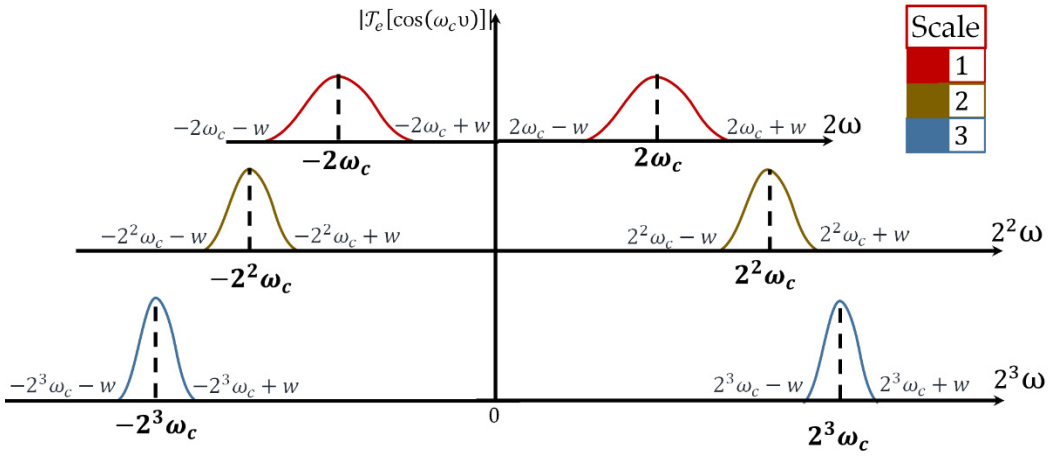

Figure 6. Dyadic frequency spectrum for $cos(\omega_c v)$.

5. Conclusions

This paper presents six contributions to knowledge in the field of mathematics applied to engineering. The main objective of these contributions is to show the mathematical foundations for creating an environment on the $\mathcal{T}_e$ domain.

The combination of the two windows forming the $\mathcal{T}_e$ window provides maximum noise attenuation. Being able to have a window like the one mentioned above allows the $\mathcal{T}_e$ transform to have an inverse. This means that an absolutely integrable function can be recovered to which the $\mathcal{T}_e$ transform has been applied, making its use more attractive like an integral transform.

Recovering a function from its integral representation in the dyadic frequency spectrum is of great importance in various fields of science, engineering, and technology, such as audio and music processing, engineering, data processing, and time series analysis, among others.

On the other hand, having a new definition of the $\mathcal{T}_e$ transform in two parameters maximizes the precision of mathematical analysis. Furthermore, it provides a new bi-dimensional approach for analyzing functions, referred to as scale frequency. This approach allows us to understand how scale varies as a function of frequency.

The uniqueness theorem emphasizes the significant importance of making it clear that the recovery of a function from its dyadic frequency spectrum is only possible through the $\mathcal{T}_e$ transform.

From the examples, we observe that having a multi-sensitive spectrum (dyadic frequency spectrum) enables the isolation of frequency components, allowing for their identification. This strengthens applications aimed at fault diagnosis, which is crucial in fields such as mechanical engineering and seismic analysis.

Having the $\mathcal{T}_e$ transform in $\mathrm{L}^1(\mathbb{R})$ allows us to validate recovery theorems and all the theorems that rely on the $\mathcal{T}_e$ transform inversion theorem. In applications where it is desirable to modify spectral characteristics of functions, it is of great importance to subsequently return the function to the time or spatial domain.

In future studies, we will investigate the energy preservation of a signal after applying the $\mathcal{T}_e$ transform. We will delve into the reconstruction of functions from the $\mathcal{T}_e$ transform

and assess its error. We will also conduct a computational complexity analysis to determine its effectiveness in noise attenuation within the fields of engineering and technology. Furthermore, we will employ the $\mathcal{T}_e$ transform in fault detection applications.

Author Contributions: Conceptualization, E.T.-C.; methodology, E.T.-C.; formal analysis, D.S.-J., J.M.N.-J., D.V.-S. and L.C.-S.; investigation, J.M.N.-J. and J.C.; supervision, D.S.-J. All authors have read and agreed to the published version of the manuscript.

Funding: This research received no external funding.

Data Availability Statement: Data sharing not applicable.

Acknowledgments: The authors thank H. Seuret-Silva for the technical support in reviewing the manuscript. The work described in this paper is supported by CONACYT, Mexico.

Conflicts of Interest: The authors declare no conflict of interest.

References

1. Carrera-Avendaño, E.; Urquiza-Beltrán, G.; Trutié-Carrero, E.; Nieto-Jalil, J.M.; Carrillo-Pereyra, C.; Seuret-Jiménez, D. Detection of crankshaft faults by means of a modified Welch-Bartlett periodogram. *Eng. Fail. Anal.* **2022**, *132*, 105938. [CrossRef]
2. Trutié-Carrero, E.; Seuret-Jimenez, D.; Nieto-Jalil, J.M. A high-resolution dyadic transform for non-stationary signal analysis. *Mathematics* **2021**, *9*, 3041. [CrossRef]
3. Trutié-Carrero, E.; Seuret-Jiménez, D.; Nieto-Jalil, J.M.; Herrera-Díaz, J.C.; Cantó, J.; Escobedo-Alatorre, J.J. Detection of Background Water Leaks Using a High-Resolution Dyadic Transform. *Water* **2023**, *15*, 736. [CrossRef]
4. Seuret-Jiménez, D.; Trutié-Carrero, E.; Nieto-Jalil, J.M.; García-Aquino, E.D.; Díaz-González, L.; Carballo-Sigler, L.; Quintana-Fuentes, D.; Gaggero-Sager, L.M. Feature Extraction of a Non-Stationary Seismic–Acoustic Signal Using a High-Resolution Dyadic Spectrogram. *Sensors* **2023**, *23*, 6051. [CrossRef] [PubMed]
5. Pallotta, L.; Giunta, G.; Farina, A. DOA refinement through complex parabolic interpolation of a sparse recovered signal. *IEEE Signal Process. Lett.* **2021**, *28*, 274–278. [CrossRef]
6. Fisher, D.A. High-resolution multiproxy climatic records from ice cores, tree-rings, corals and documentary sources using eigenvector techniques and maps: Assessment of recovered signal and errors. *Holocene* **2002**, *12*, 401–419. [CrossRef]
7. Chui, C.K.; Jiang, Q.; Li, L.; Lu, J. Signal separation based on adaptive continuous wavelet-like transform and analysis. *Appl. Comput. Harmon. Anal.* **2021**, *53*, 151–179. [CrossRef]
8. Bracewell, R.N. *The Fourier Transform and Its Applications*; McGraw-Hill Series in Electrical and Computer Engineering; McGraw-Hill: New York, NY, USA, 2000.
9. Mallat, S. *A Wavelet Tour of Signal Processing*, 3rd ed.; Elsevier: Amsterdam, The Netherlands, 2009; ISBN 9780123743701.
10. Rudin, W. Some Theorems on Fourier Coefficients. *Proc. Am. Math. Soc.* **1959**, *10*, 855. [CrossRef]
11. Kelkar, S.S.; Grigsby, L.L.; Langsner, J. An Extension of Parseval's Theorem and Its Use in Calculating Transient Energy in the Frequency Domain. *IEEE Trans. Ind. Electron.* **1983**, *IE-30*, 42–45. [CrossRef]
12. Paruthiyil, S.K.; Montoya, R.; Bidram, A.; Reno, M.J. A Numerical Method for Fault Location in DC Systems Using Traveling Waves. In Proceedings of the 2021 North American Power Symposium, NAPS 2021, IEEE, College Station, TX, USA, 14–16 November 2021; pp. 1–6.
13. Wolff, T. Fourier inversion and the Plancherel theorem. In *Non Commutative Harmonic Analysis and Lie Groups*; Springer: Berlin/Heidelberg, Germany, 2003; pp. 15–22.
14. Dhaouadi, L.; Sahbani, J.; Fitouhi, A. Harmonic analysis associated to the canonical Fourier Bessel transform. *Integr. Transform. Spec. Funct.* **2021**, *32*, 290–315. [CrossRef]
15. Zhang, Y.; Li, W. Fractional Fourier transform on $\mathbb{R}^2$ and an application. *Front. Math. China* **2022**, *17*, 1181–1200. [CrossRef]
16. Tonelli, L. Sull'integrazione per parti. *Atti Accad. Naz. Lincei* **1909**, *18*, 246–253.
17. Friedman, H. A consistent Fubini-Tonelli theorem for nonmeasurable functions. *Ill. J. Math.* **1980**, *24*, 390–395. [CrossRef]
18. Yoshikawa, T.; Innes, J. *Functional Analysis*; Elsevier: Amsterdam, The Netherlands, 2013; ISBN 9780203101261.
19. Macwhinney, B. *Functional Analysis*; Springer: Berlin/Heidelberg, Germany, 2008; Volume 52, ISBN 9781405164535.
20. Apostol, T.M. *One-Variable Calculus, with an Introduction to Linear Algebra*; Blaisdell Publishing: Waltham, MA, USA, 1967; ISBN 0471000051.
21. Velleman, D.J. *How to Prove It: A Structured Approach*; Cambridge University Press: Cambridge, UK, 2019; ISBN 110842418X.
22. Puckette, S.; Seeley, R.T. *An Introduction to Fourier Series and Integrals*; Courier Corporation: North Chelmsford, MA, USA, 1968; Volume 75, ISBN 0486151794.
23. Schwab, M. Transformation of Discrete Arrays by {Daubechies} Wavelets. *SEP-Report* **1992**, 385–402.
24. Katipoğlu, O.M. Combining discrete wavelet decomposition with soft computing techniques to predict monthly evapotranspiration in semi-arid Hakkâri province, Türkiye. *Environ. Sci. Pollut. Res.* **2023**, *30*, 44043–44066. [CrossRef] [PubMed]
25. Gon, A.; Mukherjee, A. FPGA-Based Low-Cost Architecture for R-Peak Detection and Heart-Rate Calculation Using Lifting-Based Discrete Wavelet Transform. *Circuits Syst. Signal Process.* **2023**, *42*, 580–600. [CrossRef]

26. Constantin, A. *Fourier Transforms*; Courier Corporation: North Chelmsford, MA, USA, 2016; ISBN 0486685225.
27. Boehme, T.K.; Bracewell, R.N. *The Fourier Transform and Its Applications*; McGraw-Hill: New York, NY, USA, 1966; Volume 73.
28. Gaskill, J.D. *Linear Systems, Fourier Transforms, and Optics*; John Wiley & Sons: Hoboken, NJ, USA, 1978; Volume 56, ISBN 0471292885.
29. Furman, Ł.; Duch, W.; Minati, L.; Tołpa, K. Short-time Fourier transform and embedding method for recurrence quantification analysis of EEG time series. *Eur. Phys. J. Spec. Top.* **2023**, *232*, 135–149. [CrossRef]
30. Hao, T.; Jing, L.; Liu, J.; Wang, D.; Feng, T.; Zhao, A.; Li, R. Automatic Detection of Subglacial Water Bodies in the AGAP Region, East Antarctica, Based on Short-Time Fourier Transform. *Remote Sens.* **2023**, *15*, 363. [CrossRef]
31. Sklar, B. *Digital Communications*; Prentice Hall: Upper Saddle River, NJ, USA, 1985; Volume 10.

Disclaimer/Publisher's Note: The statements, opinions and data contained in all publications are solely those of the individual author(s) and contributor(s) and not of MDPI and/or the editor(s). MDPI and/or the editor(s) disclaim responsibility for any injury to people or property resulting from any ideas, methods, instructions or products referred to in the content.